Universal Drude Weights in One-dimensional Repulsive Fermi Gas

Xiangguo Yin[1,2], Dawei Niu[1], Shuang Zhang[1], Shizhong Zhang[3], Yunbo Zhang[4†], and Xi-Wen Guan[5,6*]

[1]*Institute of Theoretical Physics and State Key Laboratory of Quantum Optics and Quantum Optics Devices, Shanxi University, Taiyuan 030006, China*

[2]*Collaborative Innovation Center of Extreme Optics, Shanxi University, Taiyuan, Shanxi 030006, China*

[3]*Department of Physics and State Key Laboratory of Optical Quantum Materials, University of Hong Kong, Hong Kong, China; Hong Kong Institute of Quantum Science and Technology, University of Hong Kong, Hong Kong, China*

[4]*Zhejiang Key Laboratory of Quantum State Control and Optical Field Manipulation, Department of Physics, Zhejiang Sci-Tech University, Hangzhou 310018, China*

[5]*Innovation Academy for Precision Measurement Science and Technology, Chinese Academy of Sciences, Wuhan 430071, China*

[6]*Department of Fundamental and Theoretical Physics, Research School of Physics, Australian National University, Canberra ACT 0200, Australia*

(Received xxx; accepted manuscript online xxx)

Building on the Bethe ansatz and generalized hydrodynamics, we rigorously establish universal relations between Drude weights governing charge, spin, and heat transport and thermodynamic properties for the one-dimensional repulsive two-component continuum Fermi gas - the paradigmatic integrable Yang-Gaudin model. We analytically derive thermodynamic expressions for charge Drude weights: D_{nn}, $D_{n\sigma}$, D_{ne} (responses of particle, magnetization and heat currents to a chemical potential gradient) equal the particle density, magnetization, and temperature times entropy density, respectively, per unit mass. These relations constitute a hallmark of ballistic transport, and can be generalized to other 1D continuum integrable systems. Furthermore, we investigate spin Drude weight ($D_{\sigma\sigma}$, $D_{\sigma e}$) at zero and low temperatures. They characterize the magnetization and heat current responses to a magnetic field gradient, revealing an essential spin-charge coupling feature in quantum transport. We find that the Drude weights $D_{n\sigma}$, $D_{\sigma\sigma}$, and $D_{\sigma e}$ across the μ-H plane remarkably map out the zero-temperature phase boundary. This work fills a critical gap in the understanding of transport within integrable quantum gases and furnishes a direct theoretical foundation for future ultracold-atom experiments.

Keywords: Drude weight; Generalized hydrodynamics; Yang-Gaudin model; Ballistic transport

DOI: 10.1088/0256-307X/43/x/xxxxxx

Introduction. The Drude Weight (DW) represents a fundamental transport coefficient in condensed matter physics, characterizing the ballistic (dissipationless) component of charge, spin, energy or other conserve charge transport in quantum many-body systems[1]. Originally developed to describe charge stiffness in solid-state materials, it quantifies the ratio of mobile charge carrier density to its effective mass. Crucially, the DW serves as an important diagnostic for distinguishing metallic and insulating phases: metals exhibit finite DWs in the thermodynamic limit, while insulators show vanishing values[2,3]. In recent years, its properties have been extensively investigated within quantum integrable models[4], such as the one-dimensional (1D) XXZ spin chain[5–9], the 1D Hubbard model[10–13], and the sine-Gordon model [14].

Significant progress in understanding DWs has been made, particularly with the development of generalized hydrodynamics (GHD) for integrable systems[15–21]. For 1D interacting systems such as the Lieb-Liniger Bose gas, theoretical progress using the Thermodynamic Bethe Ansatz (TBA) has revealed elegant integral representations of DWs[22]. These representations connect DWs to quasiparticle rapidity distributions and are equivalent to current derivatives, reflecting linear response in bipartition systems subjected to small bias potentials. Experimental studies with ultracold gases, employing protocols such as constant force or bipartition setups, have validated these theoretical predictions for 1D Bose systems[23]. These experiments confirm that DWs provide a comprehensive characterization of ballistic dynamics. Furthermore, Ref. [23] experimentally demonstrated that the DW characterizing the linear response of particle current to the variation of chemical potential is directly proportional to the particle density. Theoretical advances have also established a key property: in monoatomic gases, charge DW exhibits temperature independence and scale linearly with particle density, which follows from Galilei invariance [24–27].

*Corresponding authors. Emails: † ybzhang@zstu.edu.cn; ∗ xwe105@wipm.ac.cn

©2026 Chinese Physical Society and IOP Publishing Ltd

Despite these advancements, a significant gap remains in the comprehensive understanding of DWs for 1D multi-component continuous Fermi gases, particularly those described by the Yang-Gaudin model (δ-function interacting fermions)[28–37]. Although the two-component Yang-Gaudin Fermi gas is solved by Bethe ansatz, existing literature primarily focuses on Bose gases or addresses only particle-current-related DWs[22]. A systematic derivation of DWs encompassing spin, particle, and heat transport for these Fermionic systems is notably lacking. Moreover, the behavior of these DWs across canonical and grand canonical ensembles, specifically, their dependence on interaction strength, spin polarization, and chemical potential, has not been thoroughly characterized. This represents a significant gap in the understanding of quantum transport in strongly correlated fermions.

This paper aims to fill this gap through a comprehensive investigation of DWs in 1D repulsive Fermi gases. First, we establish a general theoretical framework by deriving charge DW as thermodynamic quantities using two complementary approaches: a linear response form under small chemical potential gradients (via generalized hydrodynamics) and an integral representation in rapidity space (via the TBA equations). This combined approach ensures the consistency and reliability of our theoretical results. Second, we systematically characterize the spin DWs in both canonical and grand canonical ensembles, revealing how key parameters, including interaction strength, spin polarization, and chemical potential, govern the particle, magnetization, and heat related DWs in these strongly correlated Fermi systems.

The Yang-Gaudin Model and its equilibrium state. We consider the 1D δ-function interacting spin-1/2 Fermi gas, widely known as the Yang-Gaudin model[28,29]. This exactly solvable system describes N fermions interacting via a point-like potential with Hamiltonian:

$$H = -\frac{\hbar^2}{2m}\sum_{i=1}^{N}\frac{\partial^2}{\partial x_i^2} + g_{1\mathrm{D}}\sum_{i<j}\delta\left(x_i - x_j\right) - \mu N - HM^z, \tag{1}$$

in which the first term is the kinetic energy, the second term is the interaction energy between particles with different spins, the last two terms are the potential energies, m is the particle mass, x_i denotes spatial coordinate, and $g_{1\mathrm{D}} = \hbar^2 c/m$ characterizes the interaction strength.

The system comprises $N_\uparrow$ spin-up and $N_\downarrow$ spin-down fermions, with total particle number $N = N_\uparrow + N_\downarrow$ and magnetization $M^z = (N_\uparrow - N_\downarrow)/2$. The chemical potential μ and magnetic field H serve as external thermodynamic potentials that couple to particle number and magnetization, respectively. This Bethe ansatz solvable model provides a powerful framework for analyzing many-body properties. Setting $\hbar = 1$, we define the particle density $n = N/L$ and magnetization density $m^z = M^z/L$, where L is the system length. These densities are essential for characterizing transport properties in quantum many-body systems.

In the thermodynamic limit, the equilibrium state is characterized by the pseudoenergies $\epsilon_1(k)$ and $\epsilon_{2,l}(k)$, which satisfy the Yang–Yang integral equations [30]

$$\begin{aligned}\epsilon_1(k) &= \frac{k^2}{2m} - \mu - \frac{H}{2} - T\sum_{l=1}^{\infty}\phi_l * \ln\!\left(1 + e^{-\epsilon_{2,l}/T}\right)(k),\\ \epsilon_{2,l}(k) &= lH - T\phi_l * \ln\!\left(1 + e^{-\epsilon_1/T}\right)(k)\\ &\quad + T\sum_{m=1}^{\infty}\Phi_{l,m} * \ln\!\left(1 + e^{-\epsilon_{2,m}/T}\right)(k),\end{aligned} \tag{2}$$

with kernels $\phi_l(k) = \dfrac{2lc}{\pi[(lc)^2 + 4k^2]}$, $l = 1, 2, \ldots$ and $\Phi_{l,m}$ as defined in the Supplemental Material (SM)[38]. Here the symbol $*$ denotes the convolution, defined by

$$(\phi_l * f)(k) = \int_{-\infty}^{\infty}\phi_l(k - k')\, f(k')\,\mathrm{d}k',$$

and k is the rapidity, which can also be interpreted as a generalized quasi-momentum or wave number. We truncate the spin-string sum at $l_{\max} = 5$ for numerics and have verified the convergence. The occupation numbers follow from the pseudoenergies through the Fermi–Dirac form

$$\theta_\alpha(k) = \left[1 + e^{\epsilon_\alpha(k)/T}\right]^{-1}, \tag{3}$$

where α labels the quasiparticle species: $\alpha = 1$ for the charge branch and $\alpha = (2, l)$ for the length-l spin string ($l = 1, 2, \ldots$). The particle density n, the magnetization density m^z, energy density e_0 and and total energy density e are expressed in terms of the rapidity distribution functions as

$$\begin{aligned} n &= \int_{-\infty}^{\infty}\mathrm{d}k\,\rho_1(k), \quad m^z = \frac{n}{2} - \sum_{l=1}^{\infty} l\int_{-\infty}^{\infty}\mathrm{d}k\,\rho_{2,l}(k),\\ e_0 &= \int_{-\infty}^{\infty}\mathrm{d}k\,\frac{k^2}{2m}\rho_1(k), \quad e = e_0 - \mu n - Hm^z, \end{aligned} \tag{4}$$

where $\rho_1(k)$ is the distribution function of the charge rapidity k, and $\rho_{2,l}(k)$ denotes the distribution function of the length-l spin string. The rapidity distribution functions are obtained from the total densities of states via $\rho_\alpha(k) = \theta_\alpha(k)\rho_\alpha^{\mathrm{tot}}(k)$, with the total densities defined through the dressed relation

$$\vec{q}_n^{\,\mathrm{dr}} = 2\pi\vec{\rho}^{\,\mathrm{tot}}, \tag{5}$$

where $\vec{q}_n = \{1, 0\}$ and $\vec{\rho}^{\,\mathrm{tot}} = \{\rho_1^{\mathrm{tot}}, \rho_{2,l}^{\mathrm{tot}}\}$. For any set of bare charges $\vec{q} = \{q_1(k), q_{2,l}(k)\}$, the corresponding

interaction dressed charges $\vec{q}^{\rm dr} = \{q_1^{\rm dr}(k), q_{2,l}^{\rm dr}(k)\}$ are determined by the linear integral equations

$$\begin{aligned} q_1^{\rm dr}(k) &= q_1(k) + \sum_{l=1}^{\infty} \phi_l * \left(q_{2,l}^{\rm dr}\theta_{2,l}\right)(k), \\ q_{2,l}^{\rm dr}(k) &= q_{2,l}(k) + \phi_l * \left(q_1^{\rm dr}\theta_1\right)(k) \\ &\quad - \sum_{m=1}^{\infty} \Phi_{l,m} * \left(q_{2,m}^{\rm dr}\theta_{2,m}\right)(k). \end{aligned} \tag{6}$$

Finally, the derivatives of the pseudoenergies with respect to the thermodynamic potentials are directly related to the corresponding conserved quantities, namely, dressed charge density $\vec{q}_n^{\rm dr} = \partial_{-\mu}\vec{\epsilon}$, dressed magnetization $\vec{q}_\sigma^{\rm dr} = \partial_{-H}\vec{\epsilon}$, dressed momentum $\vec{q}_k^{\rm dr} = m\partial_k\vec{\epsilon}$, and dressed energy $\vec{q}_e^{\rm dr} = \partial_{1/T}\vec{\epsilon}/T$ with $\vec{q}_\sigma = \{1/2, -l\}$, $\vec{q}_k = \{k, 0\}$, $\vec{q}_e = \{k^2/2m - \mu - H/2, lH\}$. Similarly, the bare eigenvalues of the energy e_0 is defined as $\vec{q}_{e_0} = \{k^2/2m, 0\}$. These relations connect the microscopic Bethe ansatz data to the macroscopic transport coefficients.

Thermodynamic Expression of Charge DW from Tilted Chemical Potential. The charge DW characterizes ballistic transport in integrable systems and can be derived through the tilted chemical potential approach [6]. Consider a system initially in thermal equilibrium with homogeneous chemical potential, subsequently subjected to a linear potential $\mu(x) = \mathcal{F}_n x$ that induces constant force driving particles transport. The DW quantifies the linear current response [23]. It is defined by first differentiating with respect to the force at zero force and then taking the long-time limit:

$$D_{ni} = \lim_{t\to\infty} \frac{1}{t} \left.\frac{\partial j_i(t)}{\partial \mathcal{F}_n}\right|_{\mathcal{F}_n=0}, \tag{7}$$

where t is the time, and j_i denotes particle ($i = n$), magnetization ($i = \sigma$), energy ($i = e_0$) or heat ($i = e$) currents with the form

$$j_i(t) = \sum_\alpha \int_{-\infty}^{\infty} {\rm d}k\ (\vec{q}_i)_\alpha\, v_\alpha \rho_\alpha(k). \tag{8}$$

Here the effective velocity v_α are given by

$$v_\alpha = \frac{(\partial_k \vec{q}_e)_\alpha^{\rm dr}(k)}{(\partial_k \vec{q}_k)_\alpha^{\rm dr}(k)}. \tag{9}$$

The time evolution of the system follows GHD [11]

$$\left(\partial_t + v_\alpha \partial_x + m a_\alpha\, \partial_k\right) \theta_\alpha(t,k) = 0, \tag{10}$$

describing quasiparticle occupation numbers θ_α in phase (x,k) space. Here the effective acceleration a_α are given by

$$a_\alpha = \frac{\left(\vec{q}_n^{\rm dr}\partial_x\mu + \vec{q}_\sigma^{\rm dr}\partial_x H\right)_\alpha}{m(\vec{q}_n^{\rm dr})_\alpha}. \tag{11}$$

Since the occupation number is uniform at every position in coordinate space for the initial state, and GHD Eq. (10) preserve spatial translational invariance, the occupation number is independent of the spatial coordinate x at arbitrary time, such that GHD Eq. (10) simplify to:

$$\left(\partial_t + ma\,\partial_k\right)\theta_\alpha(t,k) = 0, \tag{12}$$

with the effective acceleration ($a = \mathcal{F}_n/m$). Here the effective force is $ma = \mathcal{F}_n$, representing uniform force on all quasiparticles. The above partial differential Eq. (12) can be transformed into an ordinary differential equation ${\rm d}\theta_\alpha(t,k(t))/{\rm d}t = 0$ along characteristics $k(t) = k(0) + \mathcal{F}_n t$, indicating quasiparticles undergo uniform acceleration while preserving occupation numbers:

$$\theta_\alpha(t,k) = \theta_\alpha(0, k - \mathcal{F}_n t). \tag{13}$$

Equation (13) shows that the occupation number distribution is rigidly translated in rapidity space without deformation. This follows from the fact that, under the equal-mass and homogeneous equilibrium assumptions, all quasiparticles feel the same force: microscopically they drift uniformly in rapidity space, while macroscopically the center of mass accelerates uniformly, giving a particle current that grows linearly in time. This provides a direct microscopic picture of ballistic transport in both spin and charge degrees of freedom. Spin degrees of freedom form unique spin-string bound states, leading to ballistic, diffusive, and superdiffusive transport at different temperatures.

From the relation between the occupation numbers at $t = 0$ and arbitrary time t in the above Eq. (13), the particle current at time t relates to initial state occupation numbers, yielding purely ballistic contribution:

$$j_n(t) = \frac{n}{m} t\mathcal{F}_n, \tag{14}$$

and the charge DW:

$$D_{nn} = \frac{n}{m}. \tag{15}$$

Detailed derivations are given in SM [38]. This reflects the ballistic transport behavior of charge, i.e., a dissipationless fluid of quasiparticles that is independent of interaction strength and temperature. On the other hand, the Drude weight D_{nn} can also be equivalently defined via the second derivative of the pressure [24]

$$D_{nn} = 4\,\partial_\lambda^2 p\big|_{\lambda=0,\mu,H} \tag{16}$$

in the grand canonical ensemble in which p is the pressure and λ is the potential coupled to total momentum. This expression is equivalent to the second derivative of energy in the canonical ensemble under gauge field. Following a similar procedure as in Ref. [24], we obtain the identical result given in

Eq. (15). Our system features a uniform external potential and contact interactions of the delta-function, which guarantees Galilei invariance. Consequently, the system possesses continuous translational symmetry, leading to the conservation of total momentum and ballistic transport behavior, see detailed discussion in SM [38].

The magnetization current, describing spin transport, gives:

$$D_{n\sigma} = \frac{m^z}{m}. \tag{17}$$

This spin DW also matches non-interacting systems and exhibits interaction- and temperature-independent ballistic transport.

For the energy current j_{e_0}, the corresponding Drude weight is

$$D_{ne_0} = \frac{e_0 + p}{m} = \frac{h}{m}, \tag{18}$$

where e_0 is the internal energy density, i.e., the kinetic plus interaction energy density, and $h = e_0 + p$ is the enthalpy density.

For heat transport, the heat current $j_e = j_{e_0} - \mu j_n - H j_\sigma$ leads to:

$$D_{ne} = D_{ne_0} - \mu D_{nn} - H D_{n\sigma} = \frac{Ts}{m}, \tag{19}$$

where T is the temperature and s is the entropy density, revealing that finite-temperature heat transport fundamentally relates to entropy flow. At zero temperature, D_{ne} vanishes. Increasing temperature enhances entropy, consequently increasing D_{ne}. For fixed particle density, enhanced interaction strength and polarization ($P = 2m^z/n$) reduce available microstates, and therefore decrease the entropy and D_{ne}. These results demonstrate profound connections between ballistic transport coefficients and thermodynamic quantities in integrable systems in the continuous pace.

Thermodynamic Expression of Charge DW from Rapidity-Space Integration. Starting from the current-current correlation function, the DW admits an alternative formulation in rapidity space as a symmetric matrix [22]:

$$D_{ij} = \frac{1}{T} \sum_\alpha \int \mathrm{d}k\, \rho_\alpha (1-\theta_\alpha) v_\alpha^2 (\vec{q}_i^{\,\mathrm{dr}})_\alpha (\vec{q}_j^{\,\mathrm{dr}})_\alpha, \tag{20}$$

with $i, j = n, \sigma, e$. Here we suppress the explicit dependence on the rapidity k and the integration limits ($-\infty$ to $+\infty$) in the notation. The expression (20) also can be derived rigorously from the second derivative of the energy with respect to spin and charge fluxes [13]. Incidentally, for D_{nn}, the second-order derivative of pressure (16) is equivalent to the integral formulation (20) in rapidity space [38].

Using the thermal equilibrium relation $-\partial\theta_\alpha/\partial k = 2\pi\rho_\alpha(1-\theta_\alpha)v_\alpha/T$, the above expression can be rewritten as an integral incorporating derivatives of the occupation numbers:

$$D_{ij} = -\sum_\alpha \frac{1}{2\pi} \int \mathrm{d}k\, \frac{\partial\theta_\alpha}{\partial k} v_\alpha (\vec{q}_i^{\,\mathrm{dr}})_\alpha (\vec{q}_j^{\,\mathrm{dr}})_\alpha. \tag{21}$$

For charge transport D_{nn} with $\vec{q}_n = \{1, 0\}$, applying the effective velocity relation $v_\alpha = (\vec{q}_k^{\,\mathrm{dr}})_\alpha / m (\vec{q}_n^{\,\mathrm{dr}})_\alpha$, the expression (Eq. (21)) reduces to the following simple form:

$$D_{nn} = -\sum_\alpha \frac{1}{2\pi m} \int \mathrm{d}k\, \frac{\partial\theta_\alpha}{\partial k} (\vec{q}_n^{\,\mathrm{dr}})_\alpha (\vec{q}_k^{\,\mathrm{dr}})_\alpha. \tag{22}$$

The derivatives of occupation numbers in Eq. (22) can transform into derivatives of rapidity distribution functions by differentiating the TBA integral equations related to $\rho_\alpha^{\mathrm{tot}}$ from Eq. (5). After interchanging the order of integration, applying the dressed equations (6), and integrating by parts, we obtain:

$$D_{nn} = -\frac{1}{m} \int \mathrm{d}k\, \frac{\partial\rho_1}{\partial k} k = \frac{1}{m} \int \mathrm{d}k\, \rho_1 = \frac{n}{m}, \tag{23}$$

which exactly matches the result derived from the tilted potential (Eq. (15)). This confirms the universal, interaction- and temperature-independent nature of charge transport in integrable systems. Detailed derivations are given in SM [38].

For spin transport ($D_{n\sigma}$), analogous derivation yields $D_{n\sigma} = m^z/m$, reproducing Eq. (17). For heat transport, $D_{ne} = Ts/m$, reproduces Eq. (19). Detailed derivations are given in SM [38]. Unlike charge and spin transport, heat transport depends on temperature and interactions through entropy. The rapidity-space formulation provides microscopic justification for tilted potential results, confirming the inherently ballistic nature of charge and spin transport in integrable systems, while heat transport reflects thermodynamic entropy flow.

Ground State. At zero temperature, only the length $l = 1$ string contribution remains significant for spin degrees of freedom. The occupation number θ_α equals unity within the Fermi sea and vanishes outside, rendering its derivative with respect to k a positive (negative) delta function at the negative (positive) Fermi point. Consequently, the DW (Eq. (21)) receives contributions exclusively from these Fermi points

$$D_{ij} = \frac{1}{\pi} \left(v_c Z_{i1} Z_{j1} + v_s Z_{i2} Z_{j2} \right), \quad i, j = n, \sigma, \tag{24}$$

in which $v_c = v_1(k_0)$ and $v_s = v_{2,1}(\lambda_0)$ are the sound velocities of charge and spin degrees of freedom, respectively, $Z_{i1} = (\vec{q}_i^{\,\mathrm{tr}})_1(k_0)$ and $Z_{i2} = (\vec{q}_i^{\,\mathrm{tr}})_{2,1}(\lambda_0)$. Here k_0 and λ_0 denote the positive boundaries of the

rapidity distribution functions $\rho_1(k)$ and $\rho_{2,1}(k)$ at zero temperature, respectively, determined by pseudoenergy $\epsilon_1(k_0) = \epsilon_{2,1}(\lambda_0) = 0$.

Furthermore, the Yang-Yang integral equations (2) imply $\vec{\epsilon} = \vec{q}_e^{\rm dr}$ at zero temperature, which implies heat related DWs $D_{ne} = D_{\sigma e} = D_{ee} = 0$ at zero temperature. Acoording to Eqs. (15) and (17), $D_{nn} = n/m$ and $D_{n\sigma} = m^z/m$ still work at zero temperature, and then one obtain the following two identities

$$\begin{aligned} v_c Z_{n1} Z_{n1} + v_s Z_{n2} Z_{n2} &= \pi n/m, \\ v_c Z_{n1} Z_{\sigma 1} + v_s Z_{n2} Z_{\sigma 2} &= \pi m^z/m. \end{aligned} \tag{25}$$

The compressibility matrix is defined as

$$\boldsymbol{\kappa} = \begin{pmatrix} \kappa_{nn} & \kappa_{n\sigma} \\ \kappa_{\sigma n} & \kappa_{\sigma\sigma} \end{pmatrix} = \begin{pmatrix} \frac{\partial n}{\partial \mu} & \frac{\partial n}{\partial H} \\ \frac{\partial m^z}{\partial \mu} & \frac{\partial m^z}{\partial H} \end{pmatrix}. \tag{26}$$

According to the dressed equation at zero temperature, the matrix element of compressibility can be expressed in terms of the sound velocities and $Z_{i\alpha}$

$$\kappa_{ij} = \frac{1}{\pi}\left(\frac{Z_{i1}Z_{j1}}{v_c} + \frac{Z_{i2}Z_{j2}}{v_s}\right),\ i,j \in \{n,\sigma\}. \tag{27}$$

In matrix form, the DW and compressibility have the form $\boldsymbol{D} = \boldsymbol{Z}\boldsymbol{v}\boldsymbol{Z}^{\rm T}/\pi$ and $\boldsymbol{\kappa} = \boldsymbol{Z}\boldsymbol{v}^{-1}\boldsymbol{Z}^{\rm T}/\pi$, in which the matrix $\boldsymbol{D}, \boldsymbol{Z}, \boldsymbol{v}$ are defined in SM [38]. The relation between DW and compressibility is given by sound velocity irrelated form $\boldsymbol{D} = (\boldsymbol{Z}\boldsymbol{Z}^T)\boldsymbol{\kappa}^{-1}(\boldsymbol{Z}\boldsymbol{Z}^T)/\pi^2$ and the concise form $\boldsymbol{D}\boldsymbol{\kappa}^{-1} = \boldsymbol{Z}\boldsymbol{v}^2\boldsymbol{Z}^{-1}$.

Spin DW. Analogous to the tilted chemical potential approach, the spin DW can be derived using a tilted magnetic field. The system is initially prepared in an equilibrium state, after which a linear spatial dependence magnetic field $H(x) = \mathcal{F}_\sigma x$ is imposed. The corresponding DW characterizes the asymptotic current response

$$D_{\sigma i} = \lim_{t\to\infty} \frac{1}{t} \left.\frac{\partial j_i(t)}{\partial \mathcal{F}_\sigma}\right|_{\mathcal{F}_\sigma = 0}. \tag{28}$$

While the GHD Eq. (12) maintain spatial homogeneity of occupation numbers, the effective accelerations become rapidity-dependent: $a_\alpha = \mathcal{F}_\sigma(\vec{q}_\sigma^{\rm dr})_\alpha / m(\vec{q}_n^{\rm dr})_\alpha$. This contrasts with the tilted chemical potential case where accelerations is constant. Numerical computation via the method of characteristics confirms consistency with the rapidity-space integral formulation (Eq. (20)), validating both approaches for spin transport coefficients [38].

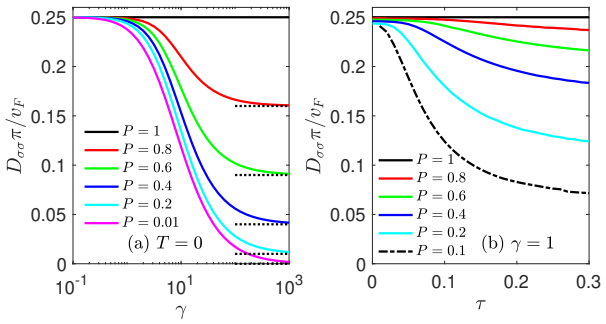

Fig. 1. DWs $D_{\sigma\sigma}$ for the ground state (a) and low temperature (b). Here $\gamma = c/n$ is the dimensionless interaction strength, P is the polarization, and $\tau = T/E_F$ is the dimensionless temperature with Fermi energy $E_F = \pi^2 n^2/2m$. Dotted lines in (a) represent analytical results in the strong interaction limits. The dimensionless interaction γ in (b) is set to be 1.

Unlike D_{nn}, the spin DW $D_{\sigma\sigma}$ depends sensitively on interactions and polarization at zero temperature. For a non-interacting Fermi gas, $D_{\sigma\sigma} = v_F/4\pi$ is independent of polarization, with the Fermi velocity given by $v_F = \pi n/m$. The dimensionless DW $D_{\sigma\sigma}/v_F$ decreases as the dimensionless interaction strength γ increases at fixed polarization (see Fig. 1(a)), demonstrating that repulsive interactions suppress spin transport. At fixed interaction strength, $D_{\sigma\sigma}/v_F$ also grows with both polarization P and magnetization density m^z. Notably, in the limit of infinite interaction strength the spin DW approaches $D_{\sigma\sigma} = v_F P^2/4\pi$. In this limit, the spin velocity vanishes, nevertheless, charge transport effects still yield a non-zero spin Drude weight for the polarized gas. This feature exposes a subtle spin-charge coupling within quantum transport, i.e. spin Drude weight remains nonvanishing even at infinite repulsion with zero spin velocity.

Fig. 1(b) shows that $D_{\sigma\sigma}$ decreases at low temperatures except ideal Fermi gas, demonstrating that temperature, similar to interactions, moderately suppresses spin transport. For strong interactions, $D_{\sigma\sigma}$ is approximately given by $\int {\rm d}k\, \rho_1 (\vec{q}_\sigma^{\rm dr})_1^2/m(\vec{q}_n^{\rm dr})_1^2$ [38].

For the fully polarized (ideal) Fermi gas with $P = 1$, the DW expression (20) contains only the one integral term with $(\vec{q}_\sigma^{\rm dr})_1 = 1/2$, leading to $D_{\sigma i} = D_{ni}/2$. This gives $D_{\sigma\sigma} = n/4m$, and $D_{\sigma e} = Ts/2m$. Applying the Sommerfeld expansion at low temperatures ($\tau = T/E_F \ll 1$) with Fermi energy $E_F = mv_F^2/2$, one obtain $D_{ne} = \left(\pi^2\tau^2/6 + \pi^4\tau^4/45\right) E_F n/m$, indicating temperature-enhanced heat related DW.

Fig. 2 shows that at relatively high temperatures, e.g. $\tau = 0.3$, $D_{\sigma e}$ increases monotonically with polarization, in agreement with the trend of $D_{\sigma\sigma}$ and in complete contrast to that of D_{ne}. At low temperatures, however, such a monotonic dependence on polarization disappears. For both very large and very small polarization, $D_{\sigma e}$ remains positive at all finite temperatures and increases monotonically with tem-

perature. In contrast, for moderate polarization, $D_{\sigma e}$ exhibits a non-monotonic behavior: it first decreases, even becoming negative at intermediate temperatures, and then increases as temperature rises further.

By Onsager reciprocity, $D_{\sigma e} = D_{e\sigma}$. They are equivalent with different interpretations: $D_{e\sigma}$ presents the magnetization-current response to a temperature gradient, while $D_{\sigma e}$ stands the heat-current response to a magnetic-field gradient. Equivalently, under $T = \mathcal{F}_T x$,

$$D_{e\sigma} = T \lim_{t\to\infty} \frac{1}{t} \frac{\partial j_\sigma(t)}{\partial \mathcal{F}_T}\bigg|_{\mathcal{F}_T=0}, \tag{29}$$

consistent with Eq. (28) via Onsager reciprocity. A negative $D_{\sigma e}$ thus means a reversal of the magnetization current under a temperature gradient (equivalently, a reversal of the heat current under a magnetic-field gradient), the inverse counterpart of the spin Seebeck effect [39].

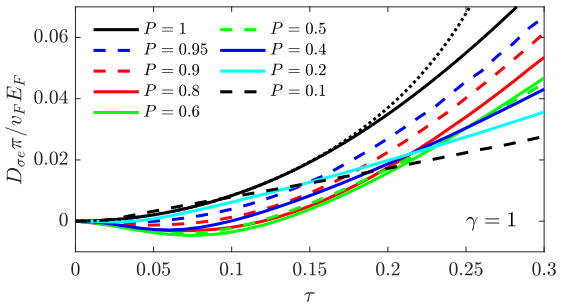

Fig. 2. DWs $D_{\sigma e}$ as functions of dimensionless temperature $\tau = T/E_F$ for different polarizations P at fixed interaction strength $\gamma = 1$. Dotted lines represent analytical results for the ideal Fermi gas at low temperature.

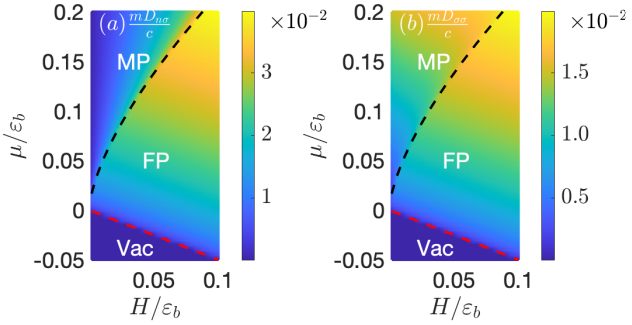

Fig. 3. Dimensionless DW (a) $mD_{n\sigma}/c$ and (b) $mD_{\sigma\sigma}/c$ in μ-H space. The black and red dashed-lines dominate the boundaries of three quantum phases: MP, FP, and Vac at zero temperature. Here $\varepsilon_b = c^2/2m$, $T/\varepsilon_b = 4 \times 10^{-4}$.

DW as indicators of zero-temperature phase boundary. In the grand canonical ensemble, Fig. 3 presents $D_{n\sigma}$ and $D_{\sigma\sigma}$ in the μ-H space at low temperatures. In the vacuum state (Vac) , since there are almost no particles, both $D_{n\sigma}$ and $D_{\sigma\sigma}$ are zero. As μ and H increase, the particle number density rises accordingly, thereby driving $D_{n\sigma}$ and $D_{\sigma\sigma}$ to increase from zero to non-zero values. This indicates a phase transition (red dashed line) from Vac to the fully polarized phase (FP). For a fixed magnetic field, as the chemical potential increases further, DW exhibits a peak, which signifies the phase transition (black dashed line) from FP to the mixed phase (MP). In MP, for a fixed magnetic field, as the chemical potential increases, the particle number density rises accordingly while the polarization decreases. This causes $D_{n\sigma}$ to decrease, whereas $D_{\sigma\sigma}$ first decreases and then increases.

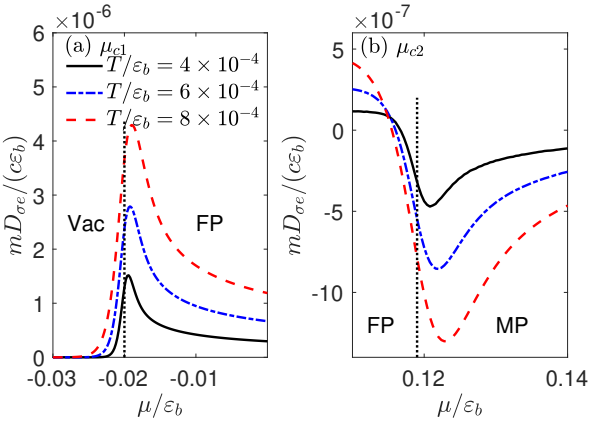

Fig. 4. Dimensionless DW $mD_{\sigma e}/(c\varepsilon_b)$ as functions of dimensional chemical potential μ/ε_b for different temperatures T at $H/\varepsilon_b = 0.04$. The critical chemical potential μ_{c1}, μ_{c2}, indicated as vertical black dashed lines, are boundaries for Vac-FP and FP-MP at zero temperature, respectively.

As is well known, the entropy at low temperatures exhibits a peak behavior near phase transitions. Consequently, D_{ne} and $D_{\sigma e}$ show a similar behavior. In Fig. 4(a), the peak position of $D_{\sigma e}$ at low temperatures is consistent with the zero-temperature Vac-FP transition point ($\mu_{c1} = -H/2$), where $D_{\sigma e} = D_{ne}/2 = Ts/(2m)$. Fig. 4(b) shows that the valley position of $D_{\sigma e}$ at low temperatures corresponds to the zero-temperature FP-MP transition point. However, on the right side of the FP-MP phase boundary, a large negative value of $D_{\sigma e}$ emerges, indicating the existence of a counterpropagating magnetization current under a temperature gradient, which is consistent with the results presented in Fig. 2.

At low temperatures, low-energy transport is dominated by real-k quasiparticle excitations coupled with length-one string excitations. In the vicinity of FP-MP phase transition, quasiparticles with spin degrees of freedom occupy only the region where the rapidity λ is small. This allows for a Taylor expansion of the pseudoenergies, the total density of states, and the dressed quantities with respect to small λ near the critical regime. One thus obtains the expression of the DWs for critical regime

$$D_{ij} = D_{\rm bg} + (\mathcal{A}_1 + \mathcal{A}_2)\, T^{1/2}\, \mathrm{Li}_{\frac{1}{2}}\left(-e^{-\epsilon_{2,1}(0)/T}\right), \tag{30}$$

with $i, j \in \{n, \sigma\}$. Here, $D_{\rm bg}$ denotes the background

contribution, which consists of the zero-temperature leading term and its analytic finite-temperature corrections. The coefficients $\mathcal{A}_1$ and $\mathcal{A}_2$, on the other hand, characterize the contributions from the charge and spin sectors, respectively. It follows that, upon subtracting the background term, the DWs D_{nn}, $D_{n\sigma}$, and $D_{\sigma\sigma}$ exhibit a distinct $T^{1/2}$ scaling behavior in the vicinity of the phase transition. The rescaled DWs, $[D_{ij} - D_{\rm bg}]T^{-1/2}$ at different temperatures intersect at the phase transition boundary, which is determined by dressed energies satisfying $\epsilon_{2,1}(0) = 0$. The detailed derivation and calculation are provided in the SM VII [38].

For the strongly interacting regime ($\gamma \gg 1$) at low temperature, we asymptotically expand the kernels of the TBA equation up to the order of $O(1/c^3)$. By iteratively solving the dressed equations (6), we can derive explicit analytical expressions for the full Drude weight matrix $(D_{nn}, D_{n\sigma}, D_{\sigma\sigma}, D_{ne}, D_{\sigma e}, D_{ee})$ at low temperatures in terms of polylogarithm functions. Detailed derivations and the complete analytical formulas are provided in the SM VIII [38].

Experimental Protocol. Motivated by the recent experiment measuring the charge DW of a 1D spinless Bose gas [23], we propose two experimental protocols to measure the DWs. The first protocol adopts the aforementioned tilted potential field and the second one takes the bipartitioning quench protocol. In the tilted chemical potential scheme, all particles are subjected to the same external force, which permits direct measurement of the charge DW. In the linear-response limit, the gradient of the tilted chemical potential is taken as $\mathcal{F}_n \to 0$ before the long-time limit. Experimentally, $\mathcal{F}_n$ is small but finite, and the time window must satisfy $\tau_{\rm micro} \ll t \ll k_F/\mathcal{F}_n$, with $\tau_{\rm micro}$ the microscopic relaxation time, so that the momentum transfer $t\mathcal{F}_n$ is much smaller than the Fermi momentum and the nonlinear response terms are negligible. In the tilted magnetic field scheme, particles with opposite spins suffer opposite forces, and this setup is suitable for measuring the spin DW. On the other hand, the second protocol examines charge and heat transport between two initially equilibrium quasi-one-dimensional subsystems with different chemical potentials, magnetic fields or temperatures. After connecting the two parts in this bipartitioning quench protocol, the corresponding DWs can be extracted by measuring particle, magnetization and heat currents. The DW is defined as the asymptotic current growth rate with respect to the vanishing bias, mathematically:

$$\begin{aligned} D_{ni} &= \lim_{\delta\mu\to 0} \frac{\partial}{\partial \delta\mu} \lim_{t\to\infty} \frac{J_i(t)}{t}, \\ D_{\sigma i} &= \lim_{\delta H\to 0} \frac{\partial}{\partial \delta H} \lim_{t\to\infty} \frac{J_i(t)}{t}, \end{aligned} \tag{31}$$

where $\delta\mu$ and δH are the chemical potential difference and magnetic field difference between the two subsystems, respectively, and $J_i(t)$ is the integral of the corresponding current over coordinate space. Using the GHD method, we obtain results consistent with the above integral form (20), validated via analytical derivation and numerical simulation, see SM [38].

Conclusion. In summary, we have analytically investigated universal spin and charge quantum transport behavior in the 1D repulsive Fermi gas known as the Yang-Gaudin model. Using the tilted chemical potential method and the generalized hydrodynamics, we have rigorously derived thermodynamic expressions for the charge and spin Drude weights. Specifically, we find that the Drude weights D_{nn}, $D_{n\sigma}$, and D_{ne}, which describe particle, spin, and heat current responses to a chemical potential gradient, equal the particle number density, magnetization, and the product of temperature and entropy density, respectively, per unit mass. These general relations also hold for other 1D integrable continuum systems with multicomponent internal spin degrees of freedom. Furthermore, we have also examined the spin Drude weight $D_{\sigma\sigma}$ at zero and low temperatures, which characterizes the magnetization-current response to a magnetic field gradient, revealing an essential spin-charge coupling feature in quantum transport. We have observed that $D_{\sigma\sigma}$ decreases substantially with increasing interparticle interaction strength and temperature. By contrast, the heat Drude weight $D_{\sigma e}$ (heat current response to a magnetic field gradient) is negative at low temperatures and turns positive at higher temperatures under moderate polarization. This sign reversal indicates inverted heat transport at low temperatures, a signature of the spin Seebeck effect. In the extreme low-temperature limit, the behaviors of $D_{n\sigma}$, $D_{\sigma\sigma}$, and $D_{\sigma e}$ across the μ-H plane effectively trace the zero-temperature phase boundary. Finally, we propose two experimental protocols for measuring these universal relations between Drude weights and thermodynamic quantities. The relations are supported by generalized hydrodynamics calculations, analytical derivations, and numerical simulations.

Acknowledgements. We acknowledge support from the Natural Science Foundation of China (NSFC) grants No. 12461160324, No. U25D8013, No. 92365202, No. 12474492, and the Innovation Program for Quantum Science and Technology Grant No. 2021ZD0302000 and 2023ZD0300404. We also acknowledge partial support from the National Key R&D Program of China under Grant No. 2022YFA1404104 and the Science Challenge Project Grant No.TZ2025017. SZ acknowledges support from HK GRF (Grant No. 17306024), CRF (Grants No. C6009-20G, No. C7012-21G, No. C4050-23GF), CRS HKU701/24 and a RGC Fellowship Award No. HKU RFS2223-7S03.

References

[1] Scalapino D J, White S R, and Zhang S C 1993 *Phys. Rev. B* **47** 7995

[2] Kohn W 1964 *Phys. Rev.* **133** A171

[3] Resta R 2018 *J. Phys.: Condens. Matter* **30** 414001.

[4] Bertini B, Heidrich-Meisner F, Karrasch C, Prosen T, Steinigeweg R, and Žnidarič M 2021 *Rev. Mod. Phys.* **93** 025003

[5] Zotos X 1999 *Phys. Rev. Lett.* **82** 1764

[6] Klümper A and Sakai K 2002 *J. Phys. A: Math. Gen.* **35** 2173

[7] Urichuk A, Öz Y, Klümper A, and Sirker J 2019 *SciPost Phys.* **6** 005

[8] Urichuk A, Sirker J, and Klümper A 2021 *Phys. Rev. B* **103** 245108

[9] Ae S and Sakai K, 2024 *J. Stat. Mech.* **2024** 033104

[10] Shirakawa T, and Jeckelmann E 2009 *Phys. Rev. B* **79** 195121

[11] Ilievski E and Nardis J D 2017 *Phys. Rev. Lett.* **119** 020602

[12] Ilievski E and Nardis J D 2017 *Phys. Rev. B* **96** 081118(R)

[13] Luo J J, Basak S, Pu H, and Guan X W 2025 *Phys. Rev. B* **112** 235414

[14] Nagy B C, Kormos M, and Takács G 2023 *Phys. Rev. B* **108** L241105

[15] Castro-Alvaredo O A, Doyon B, and Yoshimura T 2016 *Phys. Rev. X* **6** 041065.

[16] Doyon B and Yoshimura T 2017 *SciPost Phys.* **2** 014

[17] De Nardis J D, Bernard D, and Doyon B 2019 *SciPost Phys.* **6** 049

[18] Mestyán M, Bertini B, Piroli L, and Calabrese P 2019 *Phys. Rev. B* **99** 014305

[19] Scopa S, Calabrese P, and Piroli L 2022 *Phys. Rev. B* **106** 134314

[20] Wang S, Yin X G, Chen Y Y, Zhang Y B, and Guan X W 2020 *J. Phys. A: Math. Theor.* **53** 464002

[21] Nardis J D, Doyon B, Medenjak M, and Panfil M 2022 *J. Stat. Mech.* **2022** 014002

[22] Doyon B and Spohn H 2017 *SciPost. Phys.* **3** 039

[23] Schüttelkopf P, Tajik M, Bazhan N, Cataldini F, Ji S C, Schmiedmayer J, and Møller F 2026 *Science* **391** 290

[24] Göhmann F, Klümper A, and Kozlowski K K 2025 *Phys. Rev. Lett.* **135** 263401

[25] Chandak S, Petković A, and Ristivojevic Z 2026 *Phys. Rev. B* **113** 195141

[26] Liu Z Y, Yin X G, Zhang Y B, Zhang S Z and Guan X W, arXiv:2602.22009v2.

[27] Yin X G, Su Y D 2026 *Acta Phys. Sin.* **75** 200317

[28] Gaudin M 1967 *Physics Letters A* **24** 55

[29] Yang C N 1967 *Phys. Rev. Lett.* **19** 1312

[30] Lai C K 1971 *Phys. Rev. Lett.* **26** 1472

[31] Guan X W, Batchelor M T, and Lee C H 2013 *Rev. Mod. Phys.* **85** 1633

[32] Guan X W, and He P 2022 *Rep. Prog. Phys.* **85** 114001

[33] Batchelor M T, Foerster A, Guan X W, and Kuhn C C N 2010 *J. Stat. Mech.* **2010** P12014

[34] Liao Y, Rittner A S C, Paprotta T, Li W H, Partridge G B, Hulet R G, Baur S K, and Mueller E J 2010 *Nature* **467** 567

[35] Guan X W, and Ma Z Q 2012 *Phys. Rev. A* **85** 033632

[36] He W B, Chen Y Y, Zhang S Z, and Guan X W 2016 *Phys. Rev. A* **94** 031604(R)

[37] He F, Jiang Y Z, Lin H Q, Hulet R G, Pu H, and Guan X W 2020 *Phys. Rev. Lett.* **125** 190401

[38] This Supplemental Material provides rigorous proofs of the charge related Drude weight matrix with three different methods and corresponding numerical check as well as low temperature expression.

[39] Uchida K, Takahashi S, Harii K, Ieda J, Koshibae W, Ando K, Maekawa S, and Saitoh E 2008 *Nature* **455** 778